Search for High Mass Dilepton Resonances Using $10.6\,\mathrm{fb}^{-1}$ of Open Atlas Data at $\sqrt{s} = 13\,\mathrm{TeV}$

Håkon Fossheim

https://github.com/fosheimdet/FYS5555/tree/master/Project3

1 Introduction

The standard model is to date our best description of reality. It paints a picture of four fundamental forces: electromagnetism, the weak force, the strong force and gravity. So far, the force carries for all the forces have all been discovered except the hypothetical graviton, thought to mediate the gravitational force. Although the standard model has been immensely successful, it cannot be the final description of reality as it stands. One reminder of this is the fact that the angular momentum of galaxies is far to great to hold them together if not for some unknown form of matter holding them together, aptly coined dark matter. Furthermore, there is no consensus for why the forces should differ so immensely in strength, e.g. why the weak force is 10^{24} times stronger then gravity. This is referred to as the hierarchy problem. In addition, the weak force violates charge-parity symmetry by coupling only to left handed chiral particles and right handed chiral anti-particles.
Grand Unified Theories (GUTS) seek to solve some of these problems by unifying electromagnetism, the weak force and the strong force to a single gauge group. Excluding gravity is what demotes these theories from being theories of everything.
Similarly to how the electromagnetic and weak interaction unify to a single interaction (the electroweak interaction) at high energy scales, GUTS predict the same to happen for the three aforementioned forces at even higher energies.
Many of these models depend on as-of-yet undiscovered weak bosons, coined the W' and Z' bosons. Their specific properties differ depending on the model. The commonly searched for Z' bosons are the ones belonging to E6-motivated and minimal models.
The sequential standard model includes a Z'_{SSM} boson which couples to fermions in the same manner as the Z boson. Due to its simplicity, this boson proves useful as a benchmark model and is the one we aim this search at.

2 Detection of particle collisions in ATLAS

Rather than colliding two individual protons at a time, which would produce extremely few events, bunches of protons are sent at each other with 25 ns intervals at the LHC. Each bunch consists of 110 billion protons. The frequency of the bunch crossings and the number of protons contained in them determines the luminosity (L) of the particle accelerator. Events which are not of interest and that are produced in pp collisions within the current or previous bunch crossings are referred

to as pileup. Another important factor, aside from the luminosity, is the centre-of-mass energy $\sqrt{s}$, which is a measurement of how much of the energy in the collisions that is available for particle production. In a fixed-target particle accelerator where only one of the particles are accelerated, the final products of the collision must have the same momentum as that of the incoming particle. This restricts the mass of the end products. In the LHC the colliding protons have net zero momentum[1] and so in principle all of the available energy of the colliding partons could be turned into one massive particle with no momentum, which is not the case in fixed-target colliders.
The ATLAS detector has a cylindrical shape, referred to as the barrel region, which is centered around the beam pipe. It also has two flat end caps, which in conjunction with the barrel region provide almost solid angle coverage around the collision point within the beam pipe.
A solenoid magnet provide a strong magnetic field in the inner layer of the detector. The field lines are parallel to the beam line and therefore make charged particles follow curved paths in the transverse plane. If the momentum of the particle is not too high, both the charge and momentum can be discerned from the radius and bending direction of the trajectory.
Surrounding this tracking volume are the electromagnetic and hadronic calorimeters followed lastly by the muon solenoid which provide identification for muons which unlike the vast majority of particles pass through both calorimeters, depositing only ionization energy.
And so the momenta and charge of particles are determined by the tracking detector, which together with the energy measurments of the calorimeters provide means of identifying particles. When electrons hit the EM calorimeter, they create electromagnetic showers which are largely contained in said calorimeter due to dense scintillator material which reduces the mean free path of the shower particles. The electron energy can then be measured based on the size of the shower. Photons are identified as isolated energy deposits within the EM calorimeter[3].
Together with the hadron calorimeter which measures the energy of neutral hadrons, the ATLAS detector can measure every particle except neutrinos, which escape undetected. Their existence can however be inferred from momentum conservation. Because the colliding partons have no transverse momenta, the sum of the transverse momenta of all particles produces should be zero. Missing transverse momenta/energy may therefore stem from a neutrino or perhaps a particle which should have been detected, but somehow managed to escape detection.
Throughout this article we will use a right handed coordinate system with the Z-axis aligned with the beam axis. The angle between a particle's position and the z-axis is given by θ, which is related to the pseudo-rapidity[2], η, of the particle. Furthermore, the transverse direction is specified by ϕ, which is the angle the particle makes with the x-axis in the xy-plane, viz. transverse plane.
The size of jets are specified by the parameter $\Delta R = \sqrt{(\Delta\eta)^2 + (\Delta\phi)^2}$, which is a measure of the solid angle spanned by the jet and is a constant along the jet axis.

3 Event Selection

The event selection of this search is largely based on [1], but with looser selection criteria as we have less data. The events must satisfy the following:

[1] But the colliding partons may not.

[2] Defined as $\eta = -\ln[\tan(\theta/2)]$ because differences in this quantity are invariant under Lorentz boosts and so the total observed rapidity difference in the end products are the same as in the colliding quarks.

1. Require exactly two leptons of opposite charge and same flavour

2. Isolation requirements: Jets may be misidentified as leptons, or correctly identified leptons may stem from hadronic decays within jets. To filter out these scenarios, the leptons are required to be isolated. To ensure this, the E_T sum of good-quality tracks in a cone of $\Delta R = 0.20$ around the lepton candidate must be less than 20% of the lepton p_T. The lepton candidate is excluded from this sum.

3. Leptons may be categorized as being either *promt* or *non-promt*. *Promt* leptons stem from a hard scattering process in the original collision and are the decay products of heavy, short-lived particles such as the W and Z boson. As such, their vertex have a very small displacement relative to the primary vertex. *Non-promt* leptons stem from heavy flavour jets who's lifetimes are much greater. A relevant example is the b-quark decaying leptonically within a jet. Due to its mass, the leptons stemming from a b-quark decay within a jet may be produced with sufficient momenta in the direction transverse to the jet axis so as to offset their trajectories. Isolation criteria are therefore not sufficient to exclude these leptons.

   We must also require that lepton candidate tracks be consistent with the primary vertex. This is done by essentially restricting how much the lepton vertex is allowed to deviate from the primary vertex in the longitudinal and transverse directions:

   - The longitudinal impact parameter Z_0 is required to satisfy $|Z_0 \sin\theta| < 0.5\,\text{mm}$. The reason we multiply by $\sin\theta$ is that the impact parameter will be greater at smaller angles for tracks originating from the primary vertex, and so we offset this via $\sin\theta$.
   - The transverse impact parameter d_0 is the lepton track's point of closest approach to the beamline [3], i.e. its the transverse displacement. One may alternatively measure the transverse displacement by use of the impact parameter significance, defined as $|d_0/\sigma_{d_0}|$ with $d\sigma_{d_0}$ being defined by the error matrix of the track fit[2] . We require this ratio to be smaller than 3 for events to pass our selection.

4. Avoid endcap- and endcap-barrel transition regions of the EM calorimiter due to their reduced precision. Leptons within the corresponding pseudo-rapidity regions are therefore excluded:

   - electrons: $|\eta| < 2.47$ and $1.37 < |\eta| < 1.52$
   - muons: $|\eta| < 2.5$ and $1.01 < |\eta| < 1.1$

5. Lastly, in order to circumvent the Z-boson resonance peak, the reconstructed mass of the dilepton system (m_{ll}) is required to be above 110 GeV.

4 Statistical Analysis

4.1 Bayesian Inference

Bayesian inference, which we will use to determine our exclusion limits, differs quite a lot conceptually to the frequentist formulation. The main idea in the frequentist approach is to study how

[3] Prior to 2015 d_0 was calculated with respect to the position of the primary vertex.

likely it is to get the observed number of events under a background- and signal+background hypothesis and thus how confidently we can reject either one of these, which respectively constitutes a discovery or exclusion.
In the Bayesian formulation, we consider the set of all possible values the signal yield can have as well as the set of all n_{obs} one could measure. Let this be denoted by the stochastic variables s' and n'_{obs} respectively. Mapping the two-dimensional space spanned by these variables to a unit square gives figure 1, in which the possible outcomes are placed in the shown rectangles which have areas equal to their probabilities (not drawn to scale).

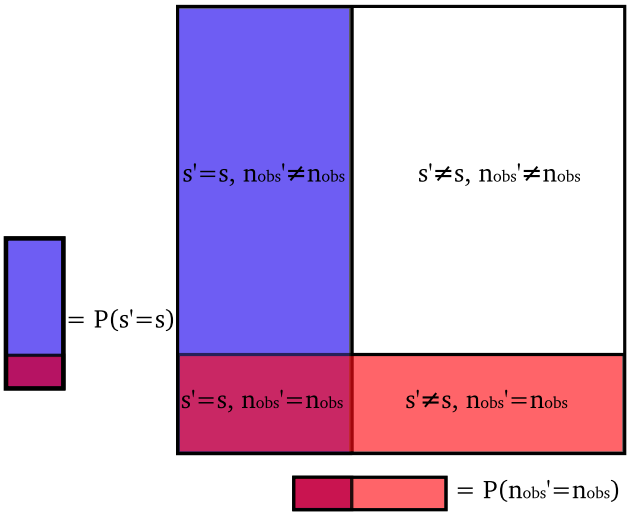

Figure (1) Visual depiction of Baye's theorem applied to our analysis.

What we are really interested in finding is the probability of getting a specific signal yield s, given that the number of observed events is n_{obs}, namely $P(s' = s|n'_{obs} = n_{obs})$. This can be thought of as the probability of getting the specific signal yield ($P(s' = s)$), represented by the combined blue and purple area times the fraction of these events that have our specific number of observed events. This fraction can be found by looking at the combined red and purple area. As seen, it is given by the probability of getting a signal yield s with n_{obs} observed events given that the number of observed events is n_{obs} ($P(n'_{obs} = n_{obs}|s' = s)$) divided by the probability of observing n_{obs} events, i.e. the ratio of the purple area to the combined purple and red area.
We therefore have

$$P(s' = s|n'_{obs} = n_{obs}) = P(s' = s) \cdot \frac{P(n'_{obs} = n_{obs}|s' = s)}{P(n'_{obs} = n_{obs})} \tag{1}$$

Which, if we drop the stochastic variable notation, can be written in the familiar form

$$P(s|n_{obs}) = \frac{P(n_{obs}|s)P(s)}{P(n_{obs})} \tag{2}$$

Here $P(s|n_{obs})$ is the so-called posterior distribution, so named because it is the our estimate of the probability of getting s after our prior estimate/belief, $P(s)$, has been updated with new ev-

idence, namely the number of observed events. The prior is often set to a flat distribution (i.e. $P(s)$ is a constant) to reflect our lack of knowledge of the process we're searching for. $P(n_{obs}|s)$ is a binomial distribution with

$$P(n_{obs}|s) = \binom{N}{n_{obs}} p^{n_{obs}}(1-p)^{n-n_{obs}} \tag{3}$$

Where N are the total number bunch crossing of our search (not just those that are triggered as events), and n_{obs} are the number of those that give events which pass the detector triggers and our analysis cuts. There is a fixed probability of any given event being categorized as an observed event if the true signal yield is s, namely p. We can show that in the limit as N goes to infinity and p goes to zero, while the number of expected observed events $\lambda = N \cdot p$ remains fixed, this distribution approaches a Poisson distribution, given by

$$P(n_{obs}|s) = \frac{\lambda^{n_{obs}} e^{-\lambda}}{n_{obs}!} \tag{4}$$

Which we call our likelihood function. Rather than using $\lambda = N \cdot p$, we can estimate the expected number of events if the true signal yield is s through Monte-Carlo simulation of the signal and background: $\lambda = b + s$.
Lastly, $P(n_{obs})$ is independent of s and so can be absorbed with $P(s)$ and $n_{obs}!$ to a single constant in front of the likelihood function:

$$P(n_{obs}|s) = C(s+b)^{n_{obs}} e^{-(s+b)} \tag{5}$$

Now we have what we need to calculate exclusion limits.
The exclusion limit is defined as the signal strength, s_{up}, above which there is only a 5% chance to observe N_{obs} events if the true signal actually is greater than or equal to s_{up}, for a given number of background events.
It is found by integrating the posterior distribution in the following manner:

$$\int_0^{s_{up}} P(s|n_{obs})ds = 0.95 \tag{6}$$

The only parameters we can have any effect on are the number of observed events and the background. The number of observed events depends both on the trigger conditions of the detector and the cuts we perform in our analysis[4]. Once we have decided on the optimal analysis cuts, the only source of potential concern regarding the final exclusion limit comes from the background. The background is estimated through Monte-Carlo simulations and has an uncertainty associated with it. We can model the background as being normally distributed with an expectation value equal to the single bin count of the background generated for our analysis, $\bar{b}$, with a standard deviation of δb.
We therefore have to adjust the posterior with a term that takes this into account. We now get a joint posterior distribution, given by

$$P(n_{obs}|s,b) = \frac{P(n_{obs}|s)P(s)P(b)}{P(n_{obs})} = C(s+b)^{n_{obs}} e^{-(s+b)} e^{-\frac{(b-\bar{b})^2}{2(\delta b)^2}} \tag{7}$$

[4]Which consists of event selection and which histogram cuts.

We now need to integrate out the b variable, viz. marginalize the joint posterior to obtain $P(n_{obs}|s)$. The upper limit for a given n_{obs} can then be found by solving equation 6. We can be shown that if $n_{obs} = 0$, the upper limit is $s_{up} = -\ln 0.05 \approx 3$.
Now, if the final upper limits seem suspiciously high or low compared to e.g. work done by others, and we are confident we have the optimal analysis cuts, then we should be sceptical of the simulated background. To quantify how likely it is that the background indeed is the cause for say an exceptionally strong, viz. low, exclusion limit rather than our peers being wrong, we can do "pseudo-experiments".
Each pseudo-experiment is set to a background which is a certain (continuous) number of standard deviations from the background of the main experiment ($\bar{b}$). We can find s_{up} in each of these experiments, and color code those that stem from deviations of 1σ or less as green and those that stem from 2σ or less as yellow. Doing this for each Z' mass yields figure 3 , from which one can assess how trustworthy the results (the circular dots) are.

4.2 Histogram cuts

The goal of our analysis is to determine whether the number of observed events is consistent with a hypothetical Z' resonance peak and how confident we are in excluding theories which predict this signal yield.
In principle, could have made no cuts at all. We could have looked at every event triggered by the ATLAS detector during run II and made our single bin span as large as possible.
The reason this is suboptimal is the large "background" this would include. The ratio $\frac{\delta b}{\bar{b}}$ stays the same, and thus the uncertainty in background in terms of number of events increases. The excess in predicted signal events compared to background would remain the same. To exclude an excess in observed data as not stemming from the background uncertainty, the hypothetical signal yield would have to be very large. In effect, our exclusion limit increases.

We therefore try to reduce the background as much as possible through proper event selection and also by restricting our single-bin to a region of the histogram with comparatively high signal to background ratio whilst including most of the potential signal events. Now the uncertainty in the number of background events becomes smaller relative to the expected excess signal yield, and so we can set the exclusion limit lower.
When choosing the single-bin region in the histogram, the cuts were chosen to minimize the exclusion limit whilst keeping as much of the resonance peak as possible.

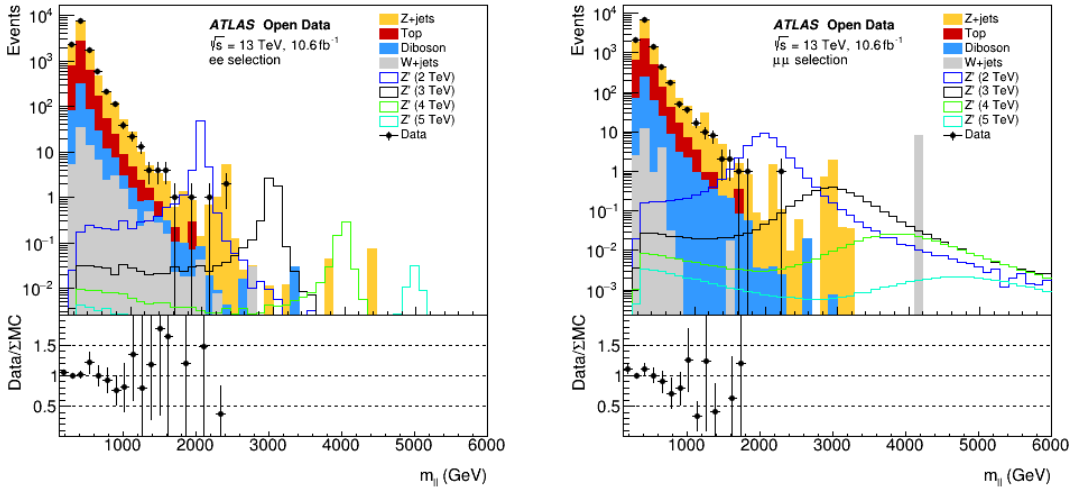

Figure (2) The upper panels show histograms of the simulated background and signal (scaled to our data) as well as our data for the $e\bar{e}$ and $\mu\bar{\mu}$ channels. The events are binned according the invariant mass of the leptons. The lower panel shows the data to background ratio to see more clearly how much the data deviates from background.

This was done separately for each Z' mass, as the peak will shift with the mass. From figure 5, it's apparent that we only have data for dilepton invariant masses up to about 2400 GeV, which is enough to contain most of the 2 TeV peak in addition to a substantial part of the 3 TeV signal. Cuts are therefore made on these signals and single-bin estimates for the exclusion limits are made, as will be described in the upcoming subsection.

4.3 Exclusion limits

The 4 TeV and 5 TeV signals have peaks far outside our region of data. Being that their signal yield in the data region is extremely small, an optimal cut on these signals would be likely to contain no data. As mentioned in 4.1, this means we can only exclude theories which predict signal strengths of $s_{up} = -\ln 0.05 \approx 3$ or higher. Since the predicted 4 TeV and 5 TeV signals lie below this limit in both channels, we can not exclude these Z' masses.
Because the simulated background is very small above our data region[5], we make cuts on the 2 TeV and 3 TeV signals based on a single m_{ll} value and count everything above this value into one bin. To determine where to cut, the expected exclusion limit[6] was calculated for 9 cut values ranging from 1900 GeV to 1100 GeV at intervals of 100 GeV. For the reasons described in subsection 4.2, we opt for the cut that gives the smallest expected exclusion limit. However, cuts that that satisfy: (observed limit/step) $\notin [100, 1000]$ are excluded to ensure a good interval.

[5] Meaning in the region above $m_{ll} = 2400$ GeV.
[6] That is to say the mean exclusion limit with respect to background variations.

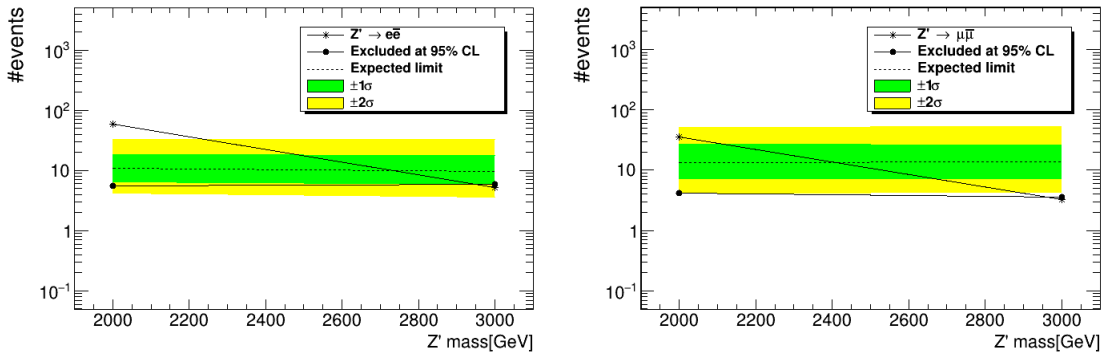

Figure (3) Exclusion limits for the ee and $\mu\mu$ channels individually. The line associated with stars show the number of expected signal events (simulated). As can be seen, this line crosses the exclusion line at about 2950 GeV for both channels. Signals corresponding to Z' with masses below this limit can therefore be excluded at 95% CL.

After finding the optimal cuts for the relevant Z' masses in the electron and muon channel, we calculate their exclusion limits s_{up}, which are shown as the black dots as seen in figure 3. Table 1 show the exact values of the exclusion limits and the exclusion bands. The bin-counts are given in table 2

Table (1) Numerical values of the exclusion limits and exlusion bands shown in figure 3.

$m_{Z'}[GeV]$	$m_{ll_{min}}[GeV]$	Channel	s_{up}	-2σ	$-\sigma$	median	$+2\sigma$	$+\sigma$
2000	1700	$e\bar{e}$	5.60	4.20	6.37	10.86	18.12	31.40
	1700	$\mu\bar{\mu}$	4.23	4.90	7.15	13.37	26.70	51.58
3000	1900	$e\bar{e}$	5.94	3.64	5.94	9.60	18.04	32.51
	1900	$\mu\bar{\mu}$	3.64	4.30	7.33	13.78	26.21	51.26

Table (2) Optimal single-bin cuts for the different $m_{Z'}$ masses in both channels and their bin counts. The error in the signal and background counts are given by the ROOT function hist.IntegralAndError().

$m_{Z'}[GeV]$	$m_{ll_{min}}[GeV]$	Channel	N_{sig}	N_{bkg}	N_{obs}
2000	1700	$e\bar{e}$	58.59 ± 0.55	9.67 ± 5.48	4
	1700	$\mu\bar{\mu}$	35.60 ± 0.06	13.51 ± 9.31	2
3000	1900	$e\bar{e}$	5.25 ± 0.05	8.33 ± 5.43	4
	1900	$\mu\bar{\mu}$	3.28 ± 0.005	12.67 ± 9.30	1

Strangely, the exclusion limits lie in the -2σ bands. When a single exclusion limit deviates this much from the expected limit, it usually indicates a statistical fluke in the generated background for this particular mass limit. However, all our exclusion limits lie in the -2σ bands. Admittedly

we have very few data points for the Z' mass, but even so, this should be a very unlikely occurrence. It may be that our event selection is sub-optimal or that there is something that was not accounted for in the code.
For completeness, we also include the produced histograms of the missing transverse energy and the transverse momentum of the leading lepton. The missing transverse energy is a parameter of interest when there are neutrinos involved in the search process, as is the case in the search for the W' boson. The transverse momentum is of interest, as leptons with very high transverse momenta are likely to be the decay products of heavy particles such as the Z' and W' bosons. Histograms of the mentioned parameters are shown in figure 4 and 5 respectively.

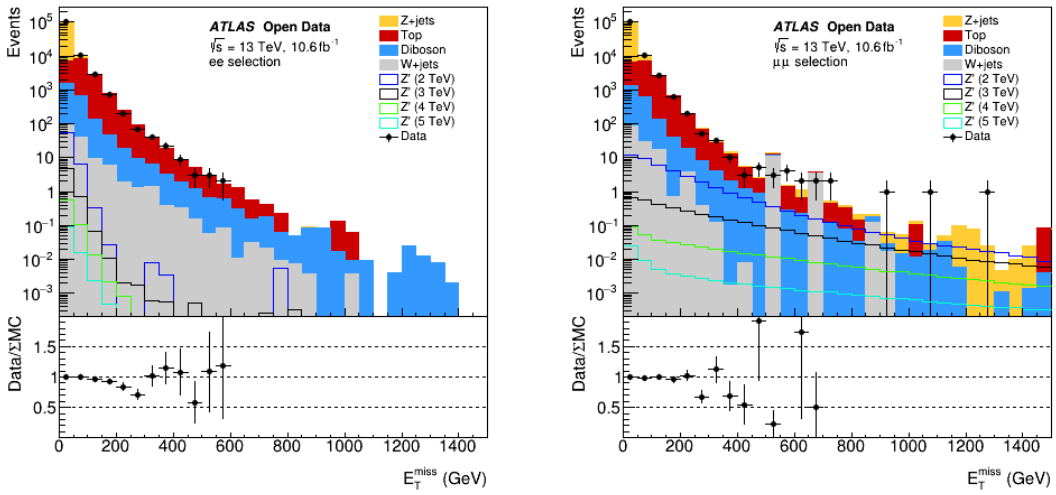

Figure (4) Missing transverse energy for the leptons in both channels.

5 Discussion

In our analysis, we saw that the number of observed events closely matched the background and we got a large deficit in observed events compared to the expected signal yields. The focus was therefore on finding exclusion limits, which we did through Bayesian inference. Had we seen an unexpected high number of events compared with background, we could have calculated the statistical significance of our single bins. This is a frequentist notion, as it relies on the concept of a background hypothesis which the Bayesian formulation does not have. Regardless, it is common practice to use statistical significance when claiming discoveries, although a Bayesian equivalent probably has been formulated.
Significance is defined based on the probability of observing the number of events we observed under the background hypothesis alone. Specifically, it calculates the area of the likelihood function where $n > n_{obs}$. The smaller this area, the less likely it is to observe n_{obs} under the background hypothesis. Where this area starts can be specified by how many standard deviations σ it is from the mean, and this is what we call the significance.

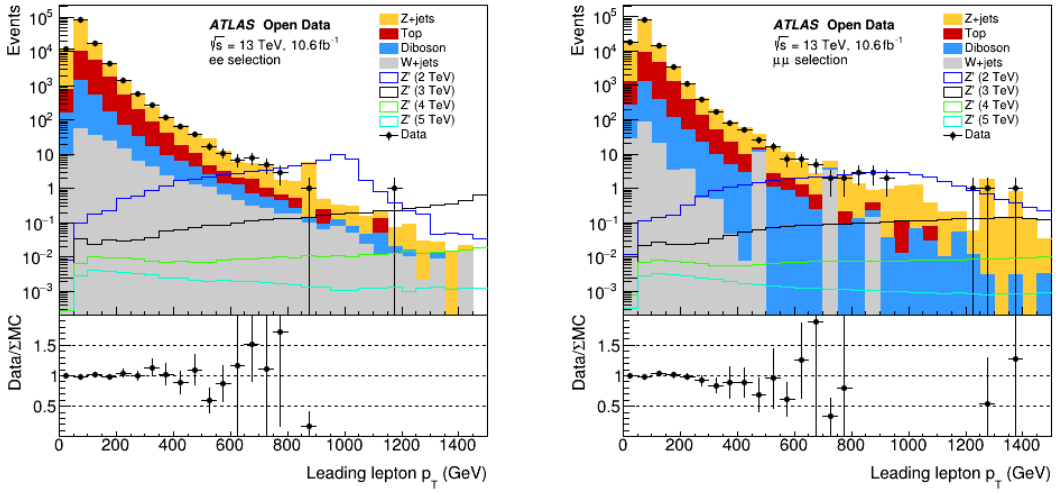

Figure (5) Transverse momenta of the leading leptons for both channels.

All four calculated exclusion limits lie in the -2σ band. The measurements may therefore be inaccurate, perhaps due to a fault in the code.

References

[1] G. Aad et al. "Search for high-mass dilepton resonances using 139 fb1 of pp collision data collected at s=13 TeV with the ATLAS detector". In: *Physics Letters B* 796 (2019), pp. 68–87. ISSN: 0370-2693. DOI: https://doi.org/10.1016/j.physletb.2019.07.016. URL: http://www.sciencedirect.com/science/article/pii/S0370269319304721.

[2] Kurt Brendlinger. *Physics with Electrons in the ATLAS Detector. First Edition.* Springer, 2018.

[3] Mark Thomson. *Modern Particle Physics. Third Edition.* Cambridge University Press, 2018.